

Optimizing Multi-objective Function for User-Defined Characteristics Relays and Size of Fault Current Limiters in Radial Networks with Renewable Energy Sources

M. Faghihi Rezaei, M. Gandomkar*, J. Nikoukar

Department of Electrical Engineering, Saveh Branch, Islamic Azad University, Saveh, Iran.

Abstract—Installing the renewable energy sources (RESs) in distribution networks changes the fault current direction, increases the fault current level and, consequently, eliminates the protection coordination between the protective devices. Overcurrent relays are among the most important protective devices in distribution networks. Proper performance of the protective system requires protection coordination between the overcurrent relays. The present paper proposes a new protection coordination scheme using digital directional overcurrent relays (DOCRs) and dual-setting digital overcurrent relays (DS-DOCRs) in the distribution network in the presence of the RESs and energy storage systems (ESSs). For this purpose, a multi-stage objective function was used. In the first stage, a weighted objective function was employed to optimize the size and location of the RESs as well as the location and impedance of the FCLs in order to reduce the loss, improve the voltage profile and decrease the variation of the feeders' currents at the connection time of the RESs. In the second stage, DOCR and DS-DOCR settings optimization, which included parameters A and B in addition to parameters I_p and TDS, was used to restore the lost protection coordination for the fault current in the shortest possible time. The simulation results on the IEEE 33-bus network in the presence of RESs using genetic algorithm and PSO algorithm method as well as DPL programming language in DIGSILENT software showed that the total operating time of digital relays and network loss were reduced and voltage profile was significantly improved.

Keywords—Dual-setting digital directional overcurrent relays, Distribution network, Power losses, Voltage profile, Fault current limiter (FCL), Protection coordination

1. INTRODUCTION

Exploitation of the traditional distribution networks is always changing to improve the energy quality and utilize new technologies [1]. Losses in distribution networks reduce the quality of the delivered energy, which is one of the most important challenges in distribution networks [2]. Electricity loss caused in distribution networks is divided into two main parts, 60% of which is lost in lines. Even a small reduction in this amount can save significant costs. A solution to reducing the losses in distribution lines is to install distributed generation (DG) sources near the consumers. By installing the DGs, the energy quality can be improved and, meanwhile, losses in network can be reduced [3]. On the other hand, these power plants are the leading cause of environmental pollution. DG implementation is an excellent option for adjusting the voltage profile, reducing loss and line congestion, improving power quality, reducing environmental pollution and generally increasing efficiency of power generation systems. With the widespread introduction of DG into distribution networks, some problems may arise regarding the proper performance of protection devices [4]. Renewable power plants can alleviate many of the problems of fossil fuel power plants. Using renewable energy reduces the effects of greenhouse gases and minimizes dependence on fossil fuels. This issue is also crucial due to the

depletion of non-renewable resources such as fossil fuels and the effort to reduce environmental pollution. One of the challenges in using these resources is their uncertainty. Most of the renewable energy sources depend on weather conditions. Among renewable energy sources, the sun is of great importance as an endless source of energy and wind energy is one of the sources that has always been available for humans. Using PV energies is unreliable due to the uncertainty of their power output because of solar radiation, panel temperature and cloud passage; also, the (v-i) characteristic of the operation surface becomes unreliable. Wind energy use due to the constant variation of wind cannot constantly generate electricity. Renewable resources are not always able to produce the same amount of power, so they are called uncertain sources [5, 6]. To minimize the losses in distribution networks, it is very important to find the optimal location and size of the DG [7]. The increasing use of DG in the distribution network, beside its numerous advantages in terms of environment and distribution network exploitation, will cause some protection problems, so that the short-circuit current level injected into the network in fault condition is very high, which results in the loss of protection coordination in the distribution network [8, 9]. Since more than 80% of the faults in the power systems occur in the distribution network, implementing appropriate protection coordination for the overcurrent relays is very important for achieving high and rapid protection in the distribution network fault condition [10–12]. For this purpose, different solutions have been proposed so far, one of which is the use of FCL along with the DG. Although FCL can have many advantages, such advantages depend on optimizing the location and size of the FCLs. In [13], DOCR parameters such as excitation current and time adjustment factor were readjusted using metaheuristic algorithms to overcome the effect of DG sources in distribution grids, restore the lost protection coordination and achieve the minimum operation time. However,

Received: 01 Apr. 2022

Revised: 24 Jul. 2022

Accepted: 08 Oct. 2022

*Corresponding author:

E-mail: gandomkar@iau-saveh.ac.ir (M. Gandomkar)

DOI: 10.22098/JOAPE.2022.10582.1757

Research Paper

©2023 University of Mohaghegh Ardabili. All rights reserved

PV LOCATION					PV SIZE					WT LOCATION					WT SIZE				
Bit 0	Bit 1	Bit 2	Bit 3	Bit 4	Bit 5	Bit 6	Bit 7	Bit 8	Bit 9	Bit 10	Bit 11	Bit 12	Bit 13	Bit 14	Bit 15	Bit 16	Bit 17	Bit 18	Bit 19

Fig. 1. RES's location and size information.

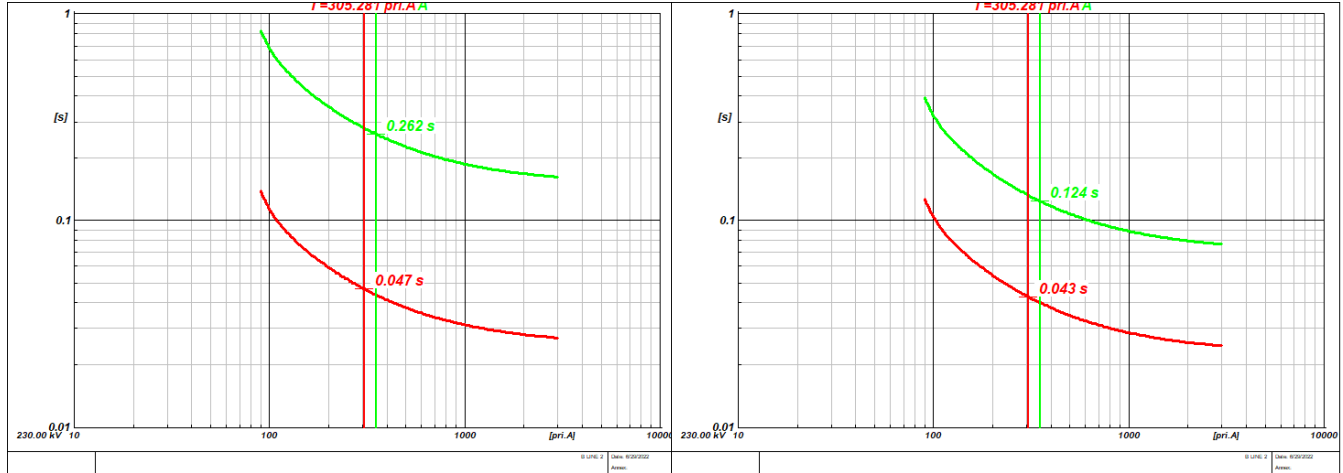


Fig. 2. (a) Protection coordination between primary and backup relay, (b) Miscoordination between primary and backup relay

given that other parameters were constant, the operation time of protective equipment did not decrease from a certain value. In [14], the results indicated using dual-setting overcurrent relays could significantly reduce coordination time interval (CTI). Moreover, it could significantly decrease the overall operation time of both primary and backup relays by maintaining coordination. It should be noted that these relays have two forward and reverse settings. Thus, the relays had two operating characteristics for forward and reverse faults. This issue could reduce the total operation time of the relays to some extent. However, the operation time of some relays increased in this study.

To date, several studies have been conducted on the use of OPC for DOCRs in the distribution network. In [15], the OPC scheme was employed in the meshed distribution network for DOCRs, the optimal solution of which was obtained through modified particle swarm optimization (PSO) algorithm. Based on the results of this paper, the presence of DG results in the loss of optimal coordination of the DOCRs and use of SFCL can reduce the fault current level. Also, since the operating time of the inverse-time overcurrent relays was inversely related to the network's current, the fault period increased. However, none of these studies have addressed determining the optimal size and location for SFCL considering the protection coordination between digital DOCRs and DS-DOCRs.

In [16], FCL was used to limit the effect of DG sources on the protection coordination of overcurrent relays. FCL was placed in series with DG sources in the event of the fault and limited the fault current to an acceptable level. Moreover, FCL showed negligible impedance under normal operating conditions of the grid and had insignificant losses. The results revealed the protection coordination was established in the distribution grid. In [17], directional overcurrent relays in the circular distribution grid were optimally adjusted using genetic algorithm. Then, the effect of installing distributed generation (DG) units on the coordination of relays was investigated. Moreover, restoring protection coordination was examined by fault current limiter (FCL) without changing the relay settings or removing DGs from the grid when there was a fault. The effect of different types of FCL on improving the coordination was evaluated.

Authors in [18] used the fault current limiter (FCL) in path with DGs to conduct the protection re-coordination. Although better results have been obtained through these optimization approaches than the linear and metaheuristic ones, they are not flexible. Numerical relays are also deployed for working on different matters. In [19], the optimal protection of circular distribution grid was examined without considering DG sources. Then, FCL was used to limit the injected fault current of DG sources and preserve the coordination between the relays by the previous settings. This method was employed to install one or two DG sources. The main problem of this method was that it could not be applied to a grid with high penetration of DG sources.

In [20], user-defined dual-setting DOCR with hybrid time and current-voltage characteristics (UDDORS-TCV) was proposed for the protection scheme. The suggested model was formulated in a constrained non-linear optimization fashion, which was tackled by MINLP solver of general algebraic modelling systems (GAMS) software. Dual setting DOCRs (DS-DOCRs) had different settings of TDS and I_p for forward and reverse directions in order to cope with the effect of reverse DG fault current contribution. The major disadvantage of time-current-voltage characteristic for UDDOCRs was the point that this characteristic depends on the magnitude of the fault voltage. The operating time of each UDDOCRs-TCV is designed in proportion to the voltage drop based on the fault event, so a large voltage drop indicated the fault was very close to the relay which can lead to loss of OPC. In [21], a protection coordination plan was investigated considering non-standard relay curves. The results indicated a reduction in the operation time of relays. However, more approaches could be examined.

In [12], a method was presented for coordinating directional overcurrent relays in order to reduce incoordination frequency of primary and backup relays using nondominated sorting genetic algorithm-II (NSGA-II). A solution should be found to achieve a reliable protective system and prevent high frequency of incoordination as well as CTI. Reducing the discrimination time of primary and backup relays as well as operation time of primary and backup relays simultaneously by introducing a novel method was among the novelties of this research. In contrast to conventional intelligent methods, the proposed method did not require weighting

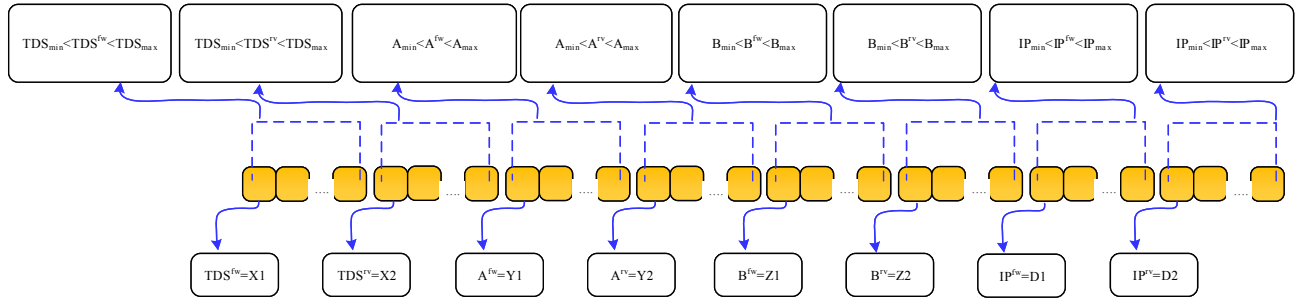


Fig. 3. Relay adjustable settings information chromosome

SFCL1 LOCATION				SFCL1 SIZE				SFCL2 LOCATION				SFCL2 SIZE				SFCL3 LOCATION				SFCL3 SIZE									
Bit 0	Bit 1	Bit 2	Bit 3	Bit 4	Bit 5	Bit 6	Bit 7	Bit 8	Bit 9	Bit 10	Bit 11	Bit 12	Bit 13	Bit 14	Bit 15	Bit 16	Bit 17	Bit 18	Bit 19	Bit 20	Bit 21	Bit 22	Bit 23	Bit 24	Bit 25	Bit 26	Bit 27	Bit 28	Bit 29

Fig. 4. SFCLs' location and size information

factors to convert the multi-objective function into an equivalent single-objective function. The effects of near- and far-end faults were considered to solve the proposed formulation. Moreover, different characteristics of overcurrent relays were considered in the program to select the best one for each relay using optimization algorithm. The results indicated the novel method had higher accuracy, flexibility and efficiency. Digital dual-setting directional overcurrent relays could be used to improve the performance of the proposed method. In [23], protection coordination and grid losses were investigated. For this purpose, a novel objective function was defined, which included constraints with different weights. This weighting determined the priority of the constraints to be met, which were obtained using some rules. The novel objective function minimized incoordination frequency, but increased operation time.

To fill the mentioned research gap, this paper first uses a weighted objective function in order to optimize the size and location of the RESs, as well as the location and impedance of the FCLs in the distribution network in order to reduce the network's line losses, improve the voltage profile and decrease the variations of the feeders' currents at the connection time of the RESs. Since RESs inject high current into the distribution network at the fault times, by locating and sizing the faults current limiters (FCLs), the effect of these RESs on the fault currents is reduced. In the proposed scheme, as these RESs are imported into the distribution network, the protection coordination between the digital DOCRs and DS-DOCRs is eliminated. The protection coordination scheme is explained for digital DOCRs and DS-DOCRs in the distribution network in the presence of RESs and ESSs. The proposed scheme minimizes the total operating time of the digital DOCRs and DS-DOCRs in the case that it is constrained with the permitted range of the setting parameters of the relays and CTI limit. In this scheme, to increase the setting flexibility of the relays in fault conditions, parameters A and B, in addition to Ip and TDS parameters, are optimized, the values of which are obtained in two fw/p and rv/b directions. To validate the proposed method, it was simulated on an IEEE-33 bus network in DigiSilent software; the genetic algorithms were used for optimization in all the stages.

2. EFFECT OF RENEWABLE ENERGY SOURCES ON DISTRIBUTION NETWORK

The use of RESs is an appropriate option for improving the voltage profiles, reducing the active and reactive power loss and environmental benefits such as reducing greenhouse gas emissions. One of the challenges in this regard is the uneven output power at different hours, which is known as uncertainty. This problem is solved using the RESs in the proposed scheme.

It should be noted that, in the proposed scheme, the capacity of each ESS is considered to be half of the RESs power generation and is installed in the same bus beside the RESs [24].

As the RESs are imported, the distribution network loss is reduced due to the shortening of the load supply path. If the location and size of the RESs are not determined properly, it will result in increased network losses.

The loss characteristic in distribution network is expressed as Equations (1) and (2):

$$P_{LOSS} = \frac{\sum_{c=1}^n (R_c I_{ac}^2)_{RES}}{(R_c I_{ac}^2)_{NO-RES}} \quad (1)$$

$$Q_{LOSS} = \frac{\sum_{c=1}^n (R_c I_{bc}^2)_{RES}}{(R_c I_{bc}^2)_{NO-RES}} \quad (2)$$

where P_{loss} is the active power loss, Q_{loss} is the reactive power loss, R_c is the line resistance, I_{ac} is the line active current, I_{bc} is the line reactive current and C is the studied line.

Importing the RESs into the distribution network changes the voltage of the buses depending on the RES capacity. If a distribution network with RESs is assumed and the location of these sources is changed, then, we will observe different effects of these sources on the distribution network. By connecting the RESs to the distribution network and installing them near the load centers, the impedance of the load supply path is reduced and, thereby, the voltage profile is improved. Since the power of the loads is supplied by the RESs, the power transmitted from the main generator to the end of the feeders is reduced. Besides, by reducing the active and reactive injected power, the voltage loss value is reduced as well. The purpose of improving the voltage profile is to bring the voltage of the buses closer to 1 p.u. The

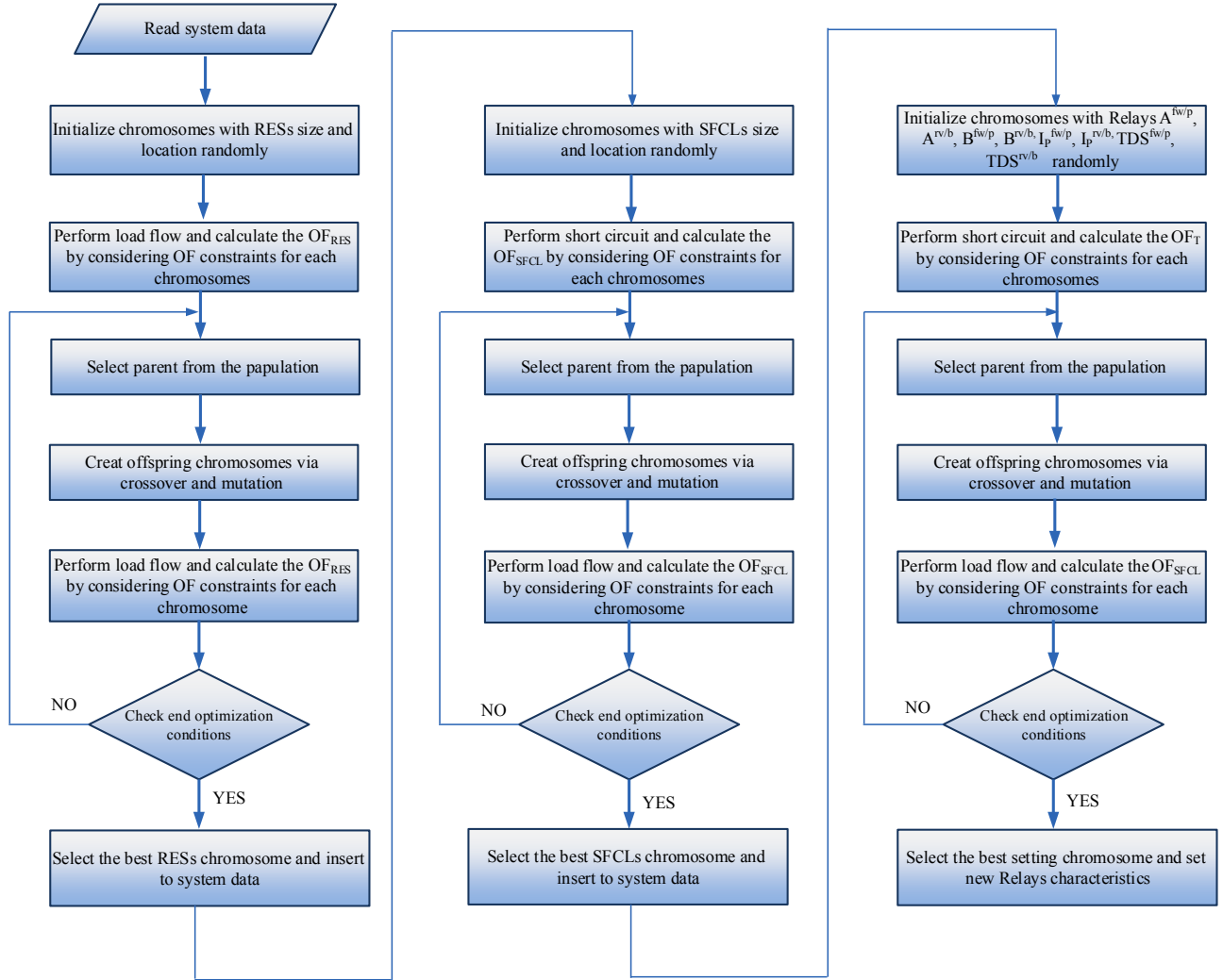


Fig. 5. The Flowchart of the proposed design
Table 1. RES_S and ESS information

Algorithm	Type RES _S , ESS _S	Installing BUS	Max Rated Power (KVA)	Active Power (KW)	Reactive Power (KVAR)
GA	PV	30	600	469	315
	WT	17	800	671	340
PSO	PV	32	600	490	296
	WT	14	800	671	338

voltage profile characteristic can be calculated using Equation (4) considering constraint (3):

$$V_{\min} \leq V_i \leq V_{\max} \quad (3)$$

$$VPI = \sum_{i=1}^n \frac{|V_i - V_{ref}|}{V_{ref}} \quad (4)$$

In the above equation, VPI indicates the voltage profile improvement characteristic, V_i indicates the voltage of the i^{th} bus, I indicates the number of buses and V_{ref} indicates the voltage of the reference bus.

The proposed objective function is a multivariable objective function that aims to optimize the size and location of the RESs in order to reduce the losses and improve the voltage profile of the buses using a weighted objective function. By connecting

RESs with different capacities to different points in the network, the values of the loss and voltage of the buses are expressed by objective function (5). Then, those values that minimize the OF_{RES} function are selected using (6) and (7) constraints.

$$OF_{RES} = \min \left(\alpha \sum_{L=1}^{\ln} P_{LOSS} + \beta \sum_{L=1}^{LN} Q_{LOSS} + \gamma \sum_{B=1}^{BN} VPI \right) \quad (5)$$

$$\sum P_{RES} \leq 0.3 \times \sum P_D \quad (6)$$

$$S_{\min} \leq S_{RES} \leq S_{\max} \quad (7)$$

In the above equation, L is the line number, B is the bus number and α , β and γ are the weighted coefficients, S_{dRES} is apparent power of each RES, P_D is power consumption and P_{RES} is RES power generation. The coefficients can be selected with regard

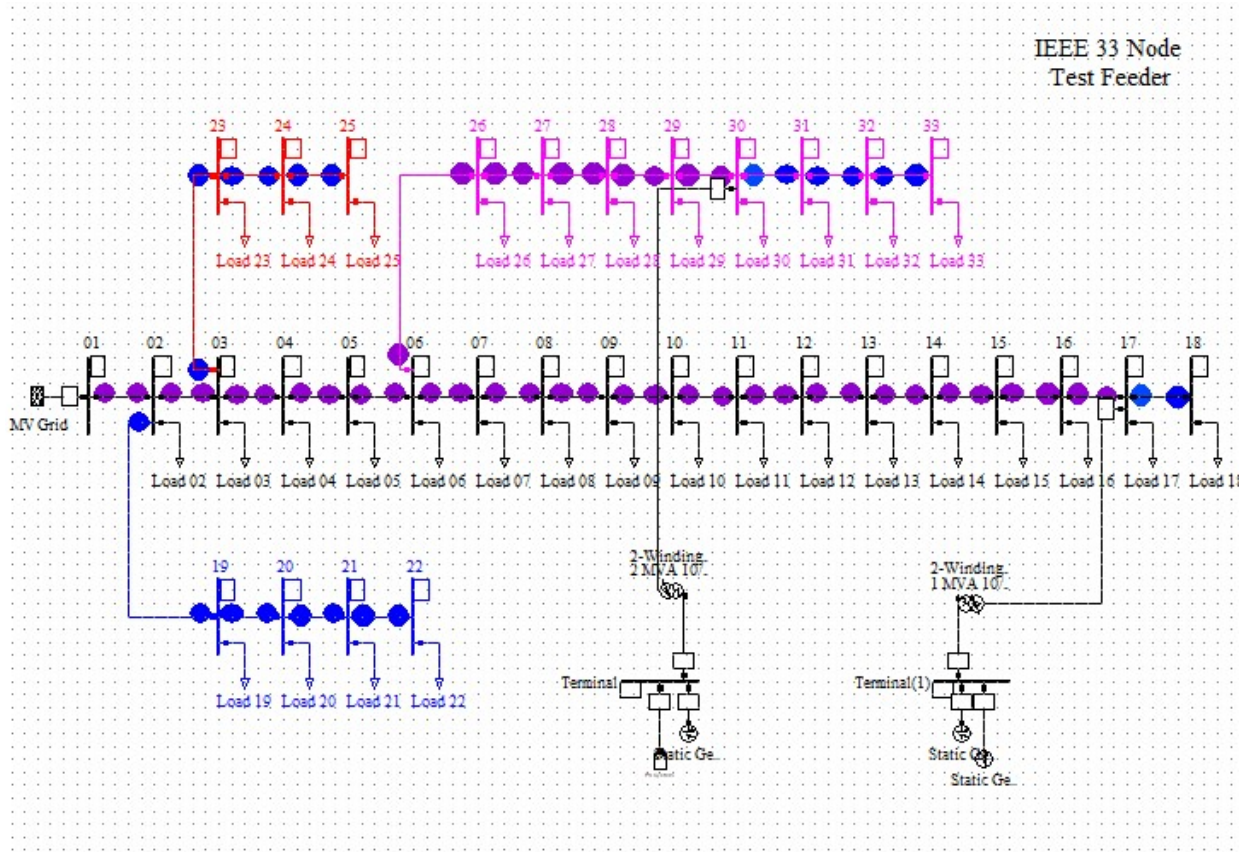


Fig. 6. Single-line diagram of the investigated 33-bus test system

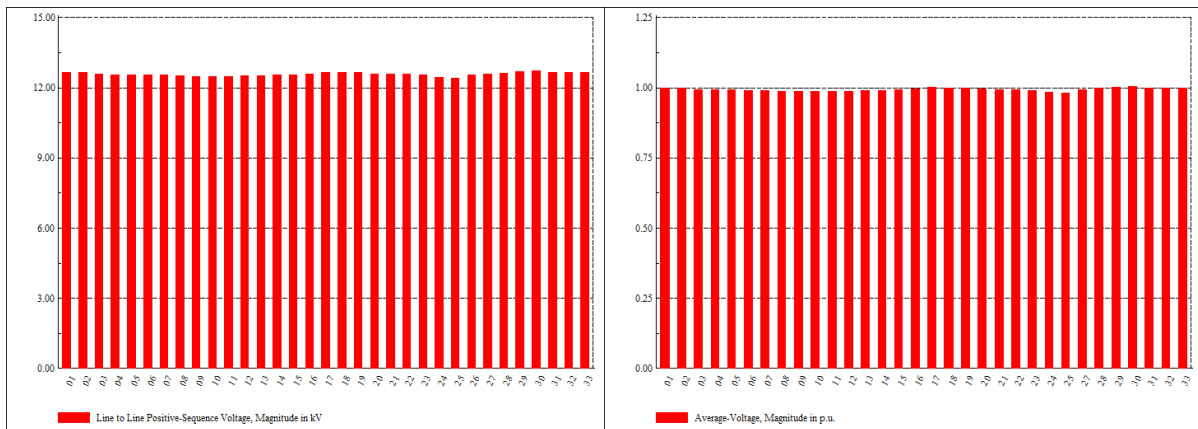


Fig. 7. All buses' voltage profile before and after installing RESs and ESS_S

to the importance and balance of each function. Accordingly, in the present paper, $\alpha=0.2$, $\beta=0.2$ and $\gamma=0.6$ are assumed. In the proposed scheme, a genetic algorithm is used to optimize the objective functions. This algorithm aims first to define variables that contain information about parameters values of the objective function variable, called chromosomes. The parameters take new values in each optimization iteration and with the values obtained in each iteration, the studied objective functions are re-examined. This process advances until the end condition, defined for the optimization problem, is reached. After reaching the end condition, appropriate values are extracted to optimize the objective functions. The length of each chromosome varies depending on the number of RESs and the degree of accuracy required. Fig. 1 shows the size and location information of the two RESs.

3. EFFECT OF RENEWABLE ENERGY SOURCES ON PROTECTION COORDINATION OF OVERCURRENT RELAYS

Today, the use of RES has become very popular due to its many benefits. Connecting renewable energy sources to the distribution network causes problems such as compromised protection coordination and increased short-circuit current levels. Therefore, protection coordination is one of the important issues that should be taken into consideration. These sources can be connected to the distribution network only on the condition that a new solution is provided to maintain the protection coordination, so that in the shortest possible time, by disconnecting the smallest part of the network, the error can be eliminated and the network can be cleaned to prevent damage to other parts and equipment. Fig. 2a shows the protection coordination between the primary and

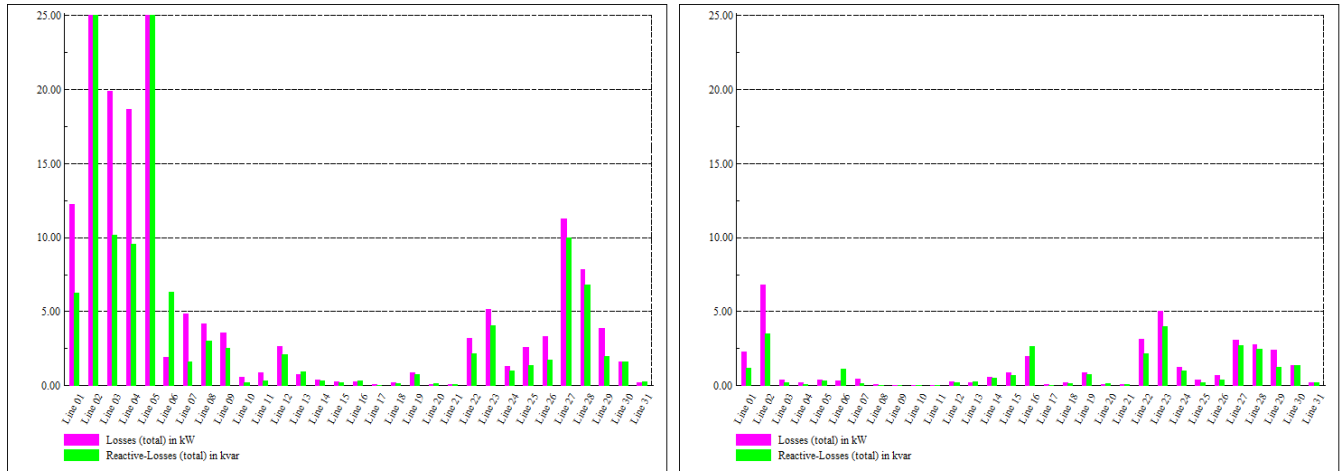


Fig. 8. All line energy losses before and after installing RESs

Table 2. Operating time in presence of PV and WT and energy storage system for 3PH fault currents

Fault Location		Operating time of relays in sec. (p=primary, b=backup) <i>fw/P</i> <i>rv/b</i>		coordination
Without RESs	F6	R ₁₁ ^{DS} :0.1619 R ₄₉ ^{DS} :0.4165 R ₁₂ ^{DS} :0.1094	R ₁₀ ^{DS} :0.4159, R ₁₃ ^{DS} :0.3664	YES
	F15	R ₂₉ ^{DS} :0.1085 R ₃₀ ^{DS} :0.1088	R ₂₈ ^{DS} :0.3435 R ₃₁ ^{DS} :0.3498	
	F26	R ₅₁ ^{DS} :0.1079 R ₅₂ ^{DS} :0.1130	R ₅₀ ^{DS} :0.3619 R ₅₃ ^{DS} :0.3635	
	F30	R ₅₉ ^D :0.1109	R ₅₈ ^{DS} :0.3559	
With RESs	F6	R ₁₁ ^{DS} :0.1018 R ₄₉ ^{DS} :0.2970 R ₁₂ ^{DS} :0.1125	R ₁₀ ^{DS} :0.2968, R ₁₃ ^{DS} :0.2475	NO
	F15	R ₂₉ ^{DS} :0.1054 R ₃₀ ^{DS} :0.1292	R ₂₈ ^{DS} :0.2924 R ₃₁ ^{DS} :0.2872	
	F26	R ₅₁ ^{DS} :0.1044 R ₅₂ ^{DS} :0.0998	R ₅₀ ^{DS} :0.2994 R ₅₃ ^{DS} :0.2858	
	F30	R ₅₉ ^D :0.1278	R ₅₈ ^{DS} :0.3258	

Table 3. SFCLs' size and location

Algorithm	Name	Installing Location	SFCL Size(Ω)
GA	SFCL1	PV	51.51
	SFCL2	WT	29.46
	SFCL3	Line 8	14.5
	SFCL4	Line 19	8.6
PSO	SFCL1	PV	62.25
	SFCL2	WT	38.5
	SFCL3	Line10	15.9
	SFCL4	Line 23	10.25

the backup relay before RES connection. Fig. 2b shows lack of protection coordination between the primary and the backup relay after RES connection.

4. PROTECTION COORDINATION OF DIGITAL DOCR AND DS-DOCR RELAYS

Backup protection is as important as the main protection. Therefore, the simultaneous reduction in the operation time of the

primary and backup relays is an essential factor for accelerating protection coordination. This is because the connection of the RESs, obtained in the first stage to the distribution network, will result in disrupted protection coordination. This section presents the optimal protection coordination for digital directional overcurrent relays in the distribution network is expressed in the presence of distributed generation resources, including photovoltaics and wind and energy storage. For this purpose, the values of parameters A, B, IP and TDS for digital DOCRs and the values of parameters $A^{fw/p}$, $A^{rv/b}$, $B^{fw/p}$, $B^{rv/b}$, $I_P^{fw/p}$, $I_P^{rv/b}$, $TDS^{fw/p}$ and $TDS^{rv/b}$ for digital DS-DOCRs are set in such a way that the total operating time of the relays is minimized in the presence of RESs and ESSs. Also, the optimal values of the mentioned parameters must be calculated. It should be noted that there is an appropriate coordination time interval (CTI) between all the primary and backup relays. Therefore, the proposed approach is modeled as follows (8):

$$OF_T = \min \left[\sum_r^N t_{op} DS - DOCR + \sum_i^M t_{op} DOCR \right] \quad \forall (i, r) \in k \quad (8)$$

Table 4. Optimal operating times of primary and backup relays in 33-bus test system based on proposed approach for 3PH fault currents (GA)

Relay	$A^{fw/p}$	$A^{rv/b}$	$B^{fw/p}$	$B^{rv/b}$	$TDS^{fw/p}$	$TDS^{rv/b}$	$I_P^{fw/p}$	$I_P^{rv/b}$	Relay	$A^{fw/p}$	$A^{rv/b}$	$B^{fw/p}$	$B^{rv/b}$	$TDS^{fw/p}$	$TDS^{rv/b}$	$I_P^{fw/p}$	$I_P^{rv/b}$
R_1^{DS}	8.5001	2.6951	0.8965	0.611	0.1015	0.1701	0.2011	0.211	R_{33}^D	3.8019	-	0.6501	-	0.3455	-	0.1077	-
R_2^{DS}	1.8999	3.1314	0.8154	0.7211	0.3486	0.3111	0.2666	0.2398	R_{34}^D	2.0892	-	0.4967	-	0.1439	-	0.0696	-
R_3^{DS}	0.1637	1.5983	0.5975	0.7416	0.2284	0.4961	0.0865	0.1099	R_{35}^D	7.1093	-	0.4476	-	0.1904	-	0.1143	-
R_4^{DS}	2.4754	4.9965	0.4682	0.5992	0.2651	0.2903	0.0598	0.0569	R_{36}^D	1.8965	-	0.5998	-	0.2967	-	0.0458	-
R_5^{DS}	1.8678	0.6899	0.7314	0.9993	0.1	0.8007	0.2148	0.1979	R_{37}^D	4.1097	-	0.8901	-	0.8097	-	0.1788	-
R_6^{DS}	2.6276	2.2831	0.8385	0.9475	0.5059	0.3501	0.1549	0.1651	R_{38}^D	0.9837	-	0.9358	-	0.4018	-	0.1967	-
R_7^{DS}	1.022	6.5973	0.6153	0.6981	0.2138	0.4531	0.0899	0.1005	R_{39}^D	5.9683	-	0.5049	-	0.2756	-	0.069	-
R_8^{DS}	8.1893	6.1167	0.8135	0.4901	0.1363	0.11	0.1098	0.0799	R_{40}^D	8.438	-	0.3966	-	0.241	-	0.122	-
R_9^{DS}	3.11	2.1644	0.6993	0.6275	0.6745	0.2506	0.1299	0.1233	R_{41}^D	3.1544	-	0.2089	-	0.3964	-	0.1681	-
R_{10}^{DS}	2.2425	8.7188	0.9991	0.8999	0.6826	0.485	0.186	0.1871	R_{42}^D	1.9548	-	0.9992	-	0.5899	-	0.0961	-
R_{11}^{DS}	2.5079	8.6011	0.6831	0.9965	0.4321	0.2403	0.2357	0.2333	R_{43}^D	6.1076	-	1	-	0.658	-	0.1374	-
R_{12}^{DS}	6.9825	0.8971	1	0.9211	0.1689	0.3474	0.2332	0.218	R_{44}^D	0.9184	-	0.7893	-	0.2508	-	0.245	-
R_{13}^{DS}	0.9719	1.8326	0.6731	0.7741	0.3792	0.8723	0.0931	0.1582	R_{45}^D	0.8999	-	0.5532	-	0.155	-	0.0556	-
R_{14}^{DS}	4.0421	1.9896	0.7954	0.6264	1	0.4895	0.2932	0.1153	R_{46}^D	1.7986	-	0.4973	-	0.3485	-	0.281	-
R_{15}^{DS}	8.7463	5.6613	0.9999	0.8489	0.1094	0.1909	0.0693	0.1671	R_{47}^D	5.694	-	0.289	-	0.4931	-	0.3043	-
R_{16}^{DS}	2.9466	7.6744	0.8327	0.3957	0.4859	0.1999	0.3583	0.0584	R_{48}^D	8.0194	-	0.4698	-	1	-	0.0683	-
R_{17}^{DS}	0.9684	1.8801	0.6681	0.9398	0.2867	0.7017	0.2877	0.0942	R_{49}^{DS}	4.9265	1.8465	0.9999	0.4541	0.273	0.821	0.2731	0.0972
R_{18}^{DS}	1.5783	4.3647	0.5637	0.9589	0.1099	0.295	0.0693	0.2683	R_{50}^{DS}	2.3854	6.9088	0.4901	0.2947	0.7333	0.1932	0.0545	0.2826
R_{19}^{DS}	5.6582	2.0193	0.8818	0.6579	0.3673	0.1	0.397	0.2839	R_{51}^{DS}	6.0186	0.9823	0.7721	0.2108	0.1904	0.5567	0.1987	0.1429
R_{20}^{DS}	1.7359	2.9472	0.5999	0.901	1	0.3109	0.0194	0.0693	R_{52}^{DS}	0.9824	1.2589	0.6905	0.8362	0.5022	0.3423	0.3158	0.0486
R_{21}^{DS}	3.7349	0.655	0.3932	0.8869	0.3855	0.3586	0.0967	0.2091	R_{53}^{DS}	0.8976	5.7943	0.8993	0.394	0.68	0.7829	0.0403	0.4015
R_{22}^{DS}	8.9147	1.0394	0.9256	0.8089	0.1071	0.921	0.149	0.0739	R_{54}^{DS}	3.6943	4.6809	1	0.7693	0.1182	0.452	0.1869	0.1801
R_{23}^{DS}	6.4626	3.0021	0.8593	1	0.4286	0.1059	0.3308	0.1948	R_{55}^{DS}	3.978	0.6999	0.4829	0.5892	0.6019	0.2259	0.4381	0.0701
R_{24}^{DS}	0.9558	4.1583	0.6835	0.3983	0.2795	1	0.1891	0.0921	R_{56}^{DS}	1.0957	5.7948	0.8902	0.6012	0.9398	0.2064	0.051	0.2495
R_{25}^{DS}	7.4621	1.9483	0.777	0.2989	0.2901	0.2059	0.1948	0.2023	R_{57}^{DS}	1.8356	2.1099	0.6654	0.5991	0.821	0.1687	0.4011	0.1839
R_{26}^{DS}	2.9586	0.9915	0.9238	0.4991	0.6976	0.3989	0.4086	0.125	R_{58}^{DS}	4.9654	5.9055	0.5731	0.821	0.1572	0.6856	0.0465	0.0898
R_{27}^{DS}	0.886	3.7079	0.5944	0.2959	1	0.1268	0.0647	0.0846	R_{59}^D	2.0928	-	0.3001	-	0.1443	-	0.098	-
R_{28}^{DS}	6.8193	0.193	0.6853	0.8376	1	0.6018	0.2093	0.2132	R_{60}^D	5.1976	-	0.2989	-	0.9909	-	0.1883	-
R_{29}^{DS}	2.8351	2.8298	0.9888	0.19487	0.701	0.3781	0.213	0.0983	R_{61}^D	0.9119	-	0.4099	-	0.789	-	0.3418	-
R_{30}^{DS}	4.3956	3.0701	0.6821	0.5899	0.2001	0.719	0.201	0.1958	R_{62}^D	7.9184	-	0.6001	-	0.355	-	0.0697	-
R_{31}^{DS}	1.8639	6.6683	0.8557	0.9999	0.6084	0.5987	0.0684	0.2701	R_{63}^D	2.7834	-	0.3969	-	0.7895	-	0.0546	-
R_{32}^{DS}	4.8492	0.8691	0.7947	0.4867	0.1772	0.1079	0.1079	0.1836	R_{64}^D	2.967	-	0.2955	-	0.1825	-	0.1953	-

The operating time for digital DOCRs can be calculated using Equation (9):

$$t = TDS \left(\frac{A}{\left(\frac{I_F}{I_P}\right)^B - 1} \right) \quad (9)$$

Regarding the point that the digital DS-DOCRs have different settings for each of the forward and reverse paths, the operating time for each of these paths is expressed as Equations (10) and (11):

$$t_{i,f}^{fw/p} = TDS_i^{fw/p} \left(\frac{A_i^{fw/p}}{\left(\frac{I_{F_{i,f}}}{I_{P_i}^{fw/p}}\right)^{B_i^{fw/p}} - 1} \right) \quad (10)$$

$$t_{r,f}^{rv/b} = TDS_r^{rv/b} \left(\frac{A_r^{rv/b}}{\left(\frac{I_{F_{r,f}}}{I_{P_r}^{rv/b}}\right)^{B_r^{rv/b}} - 1} \right) \quad (11)$$

Using constraints (12) to (19), the parameters of each of the digital DOCRs and DS-DOCRs can be set.

$$A_{\min} \leq A_r^{fw/p}, A_r^{rv/b} \leq A_{\max} \quad (12)$$

$$A_{\min} \leq A_i \leq A_{\max} \quad (13)$$

$$B_{\min} \leq B_r^{fw/p}, B_r^{rv/b} \leq B_{\max} \quad (14)$$

$$B_{\min} \leq B_i \leq B_{\max} \quad (15)$$

$$I_{P_{\min}} \leq I_{P_r}^{fw/p}, I_{P_r}^{rv/b} \leq I_{P_{\max}} \quad (16)$$

$$I_{P_{\min}} \leq I_{P_i} \leq I_{P_{\max}} \quad (17)$$

$$TDS_{\min} \leq TDS_r^{fw/p}, TDS_r^{rv/b} \leq TDS_{\max} \quad (18)$$

$$TDS_{\min} \leq TDS_i \leq TDS_{\max} \quad (19)$$

$$t_{mr,k}^{rv/b} - t_{r,k}^{fw/p} \geq CTI \quad r \in Z, mr \in MZ \quad (20)$$

$$t_{mi,k}^{rv/b} - t_{r,k}^{fw/p} \geq CTI \quad r \in Z, mi \in MY \quad (21)$$

$$t_{mr,k}^{rv/b} - t_{i,k}^{fw/p} \geq CTI \quad i \in Y, mr \in MZ \quad (22)$$

Table 5. Optimal operating times of primary and backup relays in 33-bus test system based on proposed approach for 3PH fault currents (PSO)

Relay	$A^{fw/p}$	$A^{rv/b}$	$B^{fw/p}$	$B^{rv/b}$	$TDS^{fw/p}$	$TDS^{rv/b}$	$I_p^{fw/p}$	$I_p^{rv/b}$	Relay	$A^{fw/p}$	$A^{rv/b}$	$B^{fw/p}$	$B^{rv/b}$	$TDS^{fw/p}$	$TDS^{rv/b}$	$I_p^{fw/p}$	$I_p^{rv/b}$
R_1^{DS}	6.8654	3.5463	0.7561	0.5583	0.1802	0.5762	0.2641	0.3307	R_{33}^D	5.9105	-	0.4662	-	0.421	-	0.1972	-
R_2^{DS}	5.7215	1.9785	0.7582	0.6835	0.5073	0.9864	0.2652	0.1972	R_{34}^D	0.3854	-	0.4607	-	0.2902	-	0.0896	-
R_3^{DS}	0.8854	6.1097	0.8887	0.2773	0.7683	0.4069	0.2573	0.2726	R_{35}^D	7.0186	-	0.5603	-	0.6167	-	0.2429	-
R_4^{DS}	5.1176	0.9823	0.6692	0.6108	0.1741	0.1807	0.671	0.2429	R_{36}^D	4.9661	-	0.4989	-	0.2425	-	0.5486	-
R_5^{DS}	5.0824	1.3569	0.8502	0.8461	0.6831	0.993	0.1584	0.3486	R_{37}^D	1.0176	-	0.3791	-	0.8829	-	0.1015	-
R_6^{DS}	2.8966	5.8543	0.7591	0.3264	0.894	0.1683	0.1442	0.0815	R_{38}^D	3.1983	-	0.1959	-	0.3521	-	0.3871	-
R_7^{DS}	4.6043	4.8801	1	0.8573	0.1074	0.394	0.2583	0.3871	R_{39}^D	4.978	-	0.9376	-	0.2780	-	0.1701	-
R_8^{DS}	2.958	0.7969	0.6492	0.4759	0.7583	0.1122	0.2799	0.1701	R_{40}^D	1.9857	-	0.1048	-	0.2834	-	0.3405	-
R_9^{DS}	1.0607	5.8351	0.9578	0.6583	0.7588	0.7935	0.0672	0.0495	R_{41}^D	2.0356	-	0.6890	-	0.3685	-	0.4839	-
R_{10}^{DS}	2.8361	2.5961	0.9953	0.9971	0.946	0.1092	0.2362	0.1888	R_{42}^D	5.0614	-	0.9998	-	0.5851	-	0.1898	-
R_{11}^{DS}	0.9854	5.5087	0.4863	0.451	1	0.5719	0.2778	0.2898	R_{43}^D	8.8601	-	0.3858	-	0.3809	-	0.7967	-
R_{12}^{DS}	8.674	4.9571	0.7583	0.5581	0.3681	0.921	0.2099	0.3634	R_{44}^D	2.8519	-	1	-	0.4857	-	0.449	-
R_{13}^{DS}	6.5776	1.9483	0.6573	0.859	0.964	0.2782	0.1569	0.0891	R_{45}^D	1	-	0.7731	-	0.2078	-	0.2308	-
R_{14}^{DS}	0.8996	0.8064	0.8869	0.9238	0.8087	0.6946	0.1089	0.2948	R_{46}^D	1.4754	-	0.8914	-	0.3073	-	0.3891	-
R_{15}^{DS}	7.5511	3.9269	0.7859	0.6842	0.2086	0.1403	0.2601	0.5086	R_{47}^D	5.058	-	0.8995	-	0.4908	-	0.5948	-
R_{16}^{DS}	2.0986	0.4671	0.5837	0.6663	0.8402	0.6858	0.1965	0.1647	R_{48}^D	0.8776	-	0.7361	-	0.2532	-	0.5086	-
R_{17}^{DS}	0.9954	2.7261	0.6621	0.8769	0.3069	0.9907	0.1799	0.3093	R_{49}^{DS}	3.7829	3.6510	0.5682	0.7521	0.71	0.2032	0.1647	0.1693
R_{18}^{DS}	6.312	3.1891	0.777	0.6551	0.5979	0.3257	0.2849	0.453	R_{50}^{DS}	2.43	2.6802	0.6627	0.9459	0.2152	0.1587	0.1093	0.3091
R_{19}^{DS}	2.6634	6.0913	0.9632	0.8857	0.1858	0.1064	0.385	0.216	R_{51}^{DS}	6.683	6.1083	0.7858	0.6981	1	0.2493	0.413	0.2739
R_{20}^{DS}	4.3006	0.9961	0.9946	0.7746	0.5856	0.1087	0.1509	0.1654	R_{52}^{DS}	2.7806	7.8165	0.4089	0.5771	0.4055	0.4869	0.268	0.0948
R_{21}^{DS}	1.9645	4.6175	0.5637	0.5748	0.4768	0.6056	0.2153	0.3579	R_{53}^{DS}	5.1680	0.9097	0.5931	0.4915	0.3571	0.152	0.5684	0.5921
R_{22}^{DS}	4.1041	1.0997	0.7649	0.7789	0.1701	1	0.1091	0.0357	R_{54}^{DS}	0.9531	0.9487	0.719	0.9693	0.6086	0.3559	0.1479	0.1023
R_{23}^{DS}	8.8817	0.8641	0.9736	0.9949	0.6211	0.3855	0.1584	0.3332	R_{55}^{DS}	2.0519	6.9083	0.8214	1	0.1995	0.1864	0.2871	0.168
R_{24}^{DS}	6.5638	8.0618	0.5734	0.875	0.4791	0.2071	0.1942	0.1937	R_{56}^{DS}	4.7842	0.938	0.5410	0.6809	0.2880	0.3607	0.2853	0.1846
R_{25}^{DS}	0.9910	8.8816	0.7936	0.8775	0.2953	0.3286	0.2453	0.0932	R_{57}^{DS}	3.1829	4.3544	0.3989	0.8632	0.7076	0.4806	0.518	0.3132
R_{26}^{DS}	4.1452	0.5791	0.9564	0.991	0.8576	0.2795	0.3648	0.3693	R_{58}^{DS}	5.6999	2.0548	0.8973	0.7644	0.1859	1	0.3502	0.4983
R_{27}^{DS}	8.6832	1.7426	0.5937	1	0.8591	0.2471	0.2693	0.0583	R_{59}^D	0.7948	-	0.8475	-	0.3038	-	0.6153	-
R_{28}^{DS}	2.7456	1.0572	0.5852	0.7575	0.4461	0.6016	0.1698	0.1877	R_{60}^D	5.3099	-	0.9981	-	0.4303	-	0.2671	-
R_{29}^{DS}	0.9758	5.9831	0.8472	0.9473	0.210	0.777	0.1039	0.3695	R_{61}^D	2.1055	-	0.4961	-	0.1745	-	0.1584	-
R_{30}^{DS}	1.4252	7.0581	0.2648	0.8673	0.279	0.9401	0.2968	0.475	R_{62}^D	6.2831	-	0.7275	-	0.4026	-	0.0982	-
R_{31}^{DS}	5.9841	1.0791	0.9972	0.9953	0.995	0.782	0.1921	0.2194	R_{63}^D	5.0973	-	0.5499	-	0.1301	-	0.1683	-
R_{32}^{DS}	1.7746	4.6839	0.9769	0.8093	0.8946	0.2860	0.0823	0.3966	R_{64}^D	2.1167	-	0.9863	-	0.2659	-	0.1839	-

$$t_{mi,k}^{rv/b} - t_{i,k}^{fw/p} \geq CTI \quad i \in Y, mi \in MY \quad (23)$$

In the above equations, t is the operating time of relays, TDS is the time-dial setting, I_p is the pick-up current, I_F is the fault current, A and B are the relay setting parameters, K is the set of primary/backup pairs of the relays, mr is the number of backup digital DS-DOCRs, mi is the number of backup digital DOCRs, MZ is the set of backup DS-DOCRs, MY is the set of backup DOCRs and MX is the set of backup DOCRs and DS-DOCRs.

Considering constraints (20) to (23), the protection coordination depends on the existence of sufficient time difference between the main and backup relays operation. In other words, the minimum operating time of the backup relays relative to the main relay must be more than the coordination time interval (CTI), which is usually within 0.2 to 0.5.

Fig. 3 shows the chromosome containing the DS-DOCR digital relay setting information. Of course, the authors of the article note that other optimization methods can also provide desirable values, but considering the volume of the article, the genetic method that is mostly used in this field is examined.

5. USING FCLs FOR REDUCING EFFECT OF RESS ON PROTECTION COORDINATION

One of the devices highly regarded by researchers for limiting the current of the RESSs in distribution networks in fault condition is to use the FCLs. For this purpose, in normal conditions, the network's impedance is zero, but in the case of fault occurrence in the network, the FCLs are changed to a large impedance placed on the current path of the RESSs. This large impedance is a function of the number, size and best installation location of the RESSs as well as the fault point. Therefore, having this information, we can design a suitable value for the impedance of the FCLs, in such a way that the relays can operate in the shortest possible time and the appropriate CTI between the main and backup relays operation is maintained. This impedance can be inductive, resistive or a combination of both. In the proposed scheme, to limit the fault current, a resistive superconducting fault current limiter (R-SFCL) is used due to its simple function, compact structure and small size.

The proposed objective function (24) calculates the appropriate size and location of the SFCL in order to reduce the total current passing through the protective devices of the network before and

Table 6. Dual-setting directional overcurrent relay and directional overcurrent relay operating time in presence of RESs and SFCL_S (GA)

Fault Location	Operating time of relays in sec. (p=primary, b=backup)		Fault Location	Operating time of relays in sec. (p=primary, b=backup)	
	f_w/P	rv/b		f_w/P	rv/b
F1	R ₁ ^{DS} :0.1686	-	F17	R ₃₃ ^D :0.1983	R ₃₂ ^{DS} :0.4333
	R ₂ ^{DS} :0.1715	R ₃ ^{DS} :0.4065		F18	R ₃₅ ^D :0.1869
F2	R ₃ ^{DS} :0.1364	R ₂ ^{DS} :0.3714	F19		R ₃₇ ^D :0.3591
	R ₄ ^{DS} :0.2145	R ₅ ^{DS} :0.4495		F20	R ₃₉ ^D :0.1731
F3	R ₅ ^{DS} :0.2608	R ₄ ^{DS} :0.5098	F21		R ₄₁ ^D :0.2753
	R ₆ ^{DS} :0.3275	R ₇ ^{DS} :0.5625		F22	R ₄₃ ^D :0.1963
F4	R ₇ ^{DS} :0.1796	R ₆ ^{DS} :0.4146	F23		R ₄₅ ^D :0.2508
	R ₈ ^{DS} :0.2328	R ₉ ^{DS} :0.4678		F24	R ₄₇ ^D :0.1862
F5	R ₉ ^{DS} :0.2745	R ₈ ^{DS} :0.5095	F25		R ₄₉ ^{DS} :0.2609
	R ₁₀ ^{DS} :0.1798	R ₁₁ ^{DS} :0.4408, R ₄₉ ^{DS} :0.4489		F26	R ₅₀ ^{DS} :0.2716
F6	R ₁₁ ^{DS} :0.1538	R ₁₀ ^{DS} :0.3948, R ₄₉ ^{DS} :0.3965	F27		R ₅₁ ^{DS} :0.1394
	R ₁₂ ^{DS} :0.1963	R ₁₃ ^{DS} :0.4313		F28	R ₅₂ ^{DS} :0.2370
F7	R ₁₃ ^{DS} :0.1733	R ₁₂ ^{DS} :0.4443	F29		R ₅₃ ^{DS} :0.2295
	R ₁₄ ^{DS} :0.1792	R ₁₅ ^{DS} :0.4142		F30	R ₅₄ ^{DS} :0.3164
F8	R ₁₅ ^{DS} :0.2648	R ₁₄ ^{DS} :0.4998	F31		R ₅₅ ^{DS} :0.1751
	R ₁₆ ^{DS} :0.2953	R ₁₇ ^{DS} :0.5303		F32	R ₅₆ ^{DS} :0.1932
F9	R ₁₇ ^{DS} :0.1967	R ₁₆ ^{DS} :0.4497	F31		R ₅₇ ^{DS} :0.1384
	R ₁₈ ^{DS} :0.1538	R ₁₉ ^{DS} :0.3888		F30	R ₅₈ ^{DS} :0.2530
F10	R ₁₉ ^{DS} :0.1843	R ₁₈ ^{DS} :0.4333	F30		R ₅₉ ^D :0.1944
	R ₂₀ ^{DS} :0.1692	R ₂₁ ^{DS} :0.4042		F31	R ₆₁ ^D :0.1668
F11	R ₂₁ ^{DS} :0.2165	R ₂₀ ^{DS} :0.4515	F32		R ₆₃ ^D :0.2395
	R ₂₂ ^{DS} :0.1988	R ₂₃ ^{DS} :0.4698			
F12	R ₂₃ ^{DS} :0.1951	R ₂₂ ^{DS} :0.4581			
	R ₂₄ ^{DS} :0.2146	R ₂₅ ^{DS} :0.4496			
F13	R ₂₅ ^{DS} :0.1796	R ₂₄ ^{DS} :0.4526			
	R ₂₆ ^{DS} :0.1981	R ₂₇ ^{DS} :0.4711			
F14	R ₂₇ ^{DS} :0.1568	R ₂₆ ^{DS} :0.3918			
	R ₂₈ ^{DS} :0.1943	R ₂₉ ^{DS} :0.4683			
F15	R ₂₉ ^{DS} :0.2659	R ₂₈ ^{DS} :0.5009			
	R ₃₀ ^{DS} :0.2485	R ₃₁ ^{DS} :0.4835			
F16	R ₃₁ ^{DS} :0.1863	R ₃₀ ^{DS} :0.4213			
	R ₃₂ ^{DS} :0.2463	-			

after installing the RESs. Conventionally, in such functions, the objective is to minimize the fault current limiter. However, in the proposed scheme, the objective is to reduce the total difference of the currents of the network before and after installing the RESs. For this purpose, by creating faults at different points of the network, the difference of the value of the current passing through each relay is calculated in the absence of the RESs and at the connection time of the RESs and SFCLs, considering constraint (25). Then, those SFCLs which minimize this function are selected.

$$OF_{FCL} = \min \sum_{Relay=i}^n (I_{with-RES} - I_{without-RES}) \quad (24)$$

$$Z_{min} \leq Z_{SFCL} \leq Z_{max} \quad (25)$$

The OF_{SFCL} objective function is optimized by a genetic algorithm. The chromosomes of this objective function contain SFCLs' size and location information. The length of these chromosomes varies depending on the accuracy required by the

SFCLs and their number. Fig 4 shows the information chromosome of the three SFCLs.

The performance flowchart of the proposed method is shown in Fig. 5.

6. SIMULATING THE STUDIED NETWORK

IEEE 33-bus radial distribution network, shown in Fig. 6, is simulated in DIGSILENT for evaluation. In the first stage, the optimal size and location of the RESs are found in order to reduce the line losses and improve the voltage profile. The detailed information of this network is presented in [25]. Details of the RESs are given in Table 1. By installing the RESs in different places with different power generation, it is attempted to find the most appropriate power generation capacity and location of the RESs. Then, by measuring the losses and voltage profile of the buses using the objective function OF_{RES} , the location and size of the RESs, for which the OF_{RES} is minimized, are calculated. For this purpose, the DPL programming language, which enables DIGSILENT software to program and execute the optimization codes, is used. Since the simulation is performed in DIGSILENT

Table 7. Dual-setting directional overcurrent relay and directional overcurrent relay operating time in presence of RESs and SFCL_S (PSO)

Fault Location	Operating time of relays in sec. (p=primary, b=backup)		Fault Location	Operating time of relays in sec. (p=primary, b=backup)	
	f_w/P	rv/b		f_w/P	rv/b
F1	R ₁ ^{DS} :0.1896	-	F17	R ₃₃ ^D :0.2692	R ₃₂ ^{DS} :0.5042
	R ₂ ^{DS} :0.1921	R ₃ ^{DS} :0.4271		F18	R ₃₅ ^D :0.1952
F2	R ₃ ^{DS} :0.1401	R ₂ ^{DS} :0.3751	F19		R ₃₇ ^D :0.3869
	R ₄ ^{DS} :0.2614	R ₅ ^{DS} :0.4964		F20	R ₃₉ ^D :0.1937
F3	R ₅ ^{DS} :0.2897	R ₄ ^{DS} :0.5247	F21		R ₄₁ ^D :0.2952
	R ₆ ^{DS} :0.3908	R ₇ ^{DS} :0.6258		F22	R ₄₃ ^D :0.2164
F4	R ₇ ^{DS} :0.2164	R ₆ ^{DS} :0.4514	F23		R ₄₅ ^D :0.2731
	R ₈ ^{DS} :0.2635	R ₉ ^{DS} :0.4985		F24	R ₄₇ ^D :0.1994
F5	R ₉ ^{DS} :0.1956	R ₈ ^{DS} :0.4306	F25		R ₄₉ ^{DS} :0.2706
	R ₁₀ ^{DS} :0.2683	R ₁₁ ^{DS} :0.5033, R ₄₉ ^{DS} :0.5091		F26	R ₅₀ ^{DS} :0.2841
F6	R ₁₁ ^{DS} :0.1736	R ₁₀ ^{DS} :0.4086, R ₄₉ ^{DS} :0.4098	F27		R ₅₁ ^{DS} :0.1796
	R ₁₂ ^{DS} :0.2657	R ₁₃ ^{DS} :0.5007		F28	R ₅₂ ^{DS} :0.2685
F7	R ₁₃ ^{DS} :0.1992	R ₁₂ ^{DS} :0.4342	F29		R ₅₃ ^{DS} :0.2476
	R ₁₄ ^{DS} :0.2465	R ₁₅ ^{DS} :0.4815		F30	R ₅₄ ^{DS} :0.3849
F8	R ₁₅ ^{DS} :0.2968	R ₁₄ ^{DS} :0.5318	F31		R ₅₅ ^{DS} :0.1863
	R ₁₆ ^{DS} :0.2974	R ₁₇ ^{DS} :0.5324		F32	R ₅₆ ^{DS} :0.2741
F9	R ₁₇ ^{DS} :0.2688	R ₁₆ ^{DS} :0.5038	F31		R ₅₇ ^{DS} :0.1748
	R ₁₈ ^{DS} :0.2571	R ₁₉ ^{DS} :0.4921		F30	R ₅₈ ^{DS} :0.2858
F10	R ₁₉ ^{DS} :0.1975	R ₁₈ ^{DS} :0.4465	F31		R ₅₉ ^D :0.1995
	R ₂₀ ^{DS} :0.2648	R ₂₁ ^{DS} :0.5138		F31	R ₆₁ ^D :0.1859
F11	R ₂₁ ^{DS} :0.2371	R ₂₀ ^{DS} :0.4861	F32		R ₆₃ ^D :0.2802
	R ₂₂ ^{DS} :0.2417	R ₂₃ ^{DS} :0.4907			
F12	R ₂₃ ^{DS} :0.1968	R ₂₂ ^{DS} :0.4668			
	R ₂₄ ^{DS} :0.2648	R ₂₅ ^{DS} :0.5348			
F13	R ₂₅ ^{DS} :0.1891	R ₂₄ ^{DS} :0.4591			
	R ₂₆ ^{DS} :0.2841	R ₂₇ ^{DS} :0.5540			
F14	R ₂₇ ^{DS} :0.1964	R ₂₆ ^{DS} :0.4594			
	R ₂₈ ^{DS} :0.2601	R ₂₉ ^{DS} :0.5231			
F15	R ₂₉ ^{DS} :0.1949	R ₂₈ ^{DS} :0.4649			
	R ₃₀ ^{DS} :0.2951	R ₃₁ ^{DS} :0.5651			
F16	R ₃₁ ^{DS} :0.1973	R ₃₀ ^{DS} :0.4323			
	R ₃₂ ^{DS} :0.2231	-			

software and the connection between MATLAB and DIGSILENT reduces the optimization speed, the authors decided to use DPL programming language. In each iteration of the optimization, new values are generated by the GA and, then, used. In this optimization, for the objective function OF_{RES} , the values of $\alpha=0.2$, $\beta=0.2$ and $\gamma=0.6$ are considered. Also, the total capacity of the RESs is assumed less than 1316KW (i.e., 30% of the total load of the network). For the optimization values of the GA, [26] is used. Table 1 presents the statistical results of the optimal response, obtained from GA and PSO algorithms. The PSO algorithm coded in DPL-DIGSILENT software is used for better performance.

As shown in Figs. 7 and 8, by connecting the RESs to the IEEE 33-bus distribution network, the loss of the distribution lines is reduced and the voltage profile is improved. Subsequently, the protection coordination between the protective devices of the distribution network, including the digital DOCRs and DS-DOCRs, is investigated.

The operating time of digital DOCR and DS-DOCR for main and backup relays when the RESs and ESSs are connected is

shown in Table 2.

As shown in Table 3, in the first stage, once the RESs are connected to the distribution network, the protection coordination between the relays is eliminated at some of the fault points. Therefore, the lost protection coordination should be restored in the distribution network. In the second stage, by using the R-SFCL, the effect of the RESs on the fault current is reduced. For this purpose, the installation size and location of the R-SFCL are optimized by the objective function OF_{FCL} . In the proposed scheme, four R-SFCLs are used within the impedance range of 1 to 217 Ω . The optimization results by GA and PSO algorithms are given in Table 3.

In the third stage, by optimizing the objective function OF_T , the protection coordination is restored in the shortest possible time. Also, the operating time of the protective devices, including the digital DOCRs and DS-DOCRs, with optimized settings for three-phase fault in the presence of RESs, ESSs and SFCLs are given in Tables 4 and 5. The results in Tables 6 and 7 indicate the lost protection coordination between the digital DOCRs and DS-DOCRs in the presence of the RESs and ESSs is restored

Table 8. Total operating time of digital DOCR relays and digital DS-DOCR relays using GA and PSO algorithm

Algorithm	Total operation time(sec)
GA	36.321
PSO	39.885

by using the R-SFCL and re-setting the parameters of the digital relays. The optimization constraints for the characteristics A, B, TDS and IP using [27] are driven by the following equations:

$$0.14 < A < 13.5, 0.02 < B < 1, 0.1 < TDS < 3, 0.1 < I_P < 2$$

In Table 8, the results of optimizing the total operating time of digital DOCR relays and digital DS-DOCR relays, using GA and PSO algorithms, are presented. The results show that the total operating time, obtained from the GA algorithm, is better than the PSO algorithm. Therefore, the GA algorithm can provide faster protection coordination.

7. CONCLUSION

In the present paper, the three-stage multi-objective function was developed to define the setting of relay and allocation as well as sizing of RESs, ESSs and SFCL in the distribution system. In this scheme, in the first stage, a weighted objective function was used to determine the optimal size and location of the RESs to reduce the line losses and improve the voltage profile. Then, in the second stage, it was attempted to optimize the installation size and location of the SFCLs in order to reduce the effect of the RESs on fault current and protection coordination. Afterwards, in the last stage, regarding the use of digital DOCRs and DS-DOCRs, it was attempted to optimize the settings of the relays and reduce the total operating time of the protective devices considering multiple fault points by GA and PSO. Executing the proposed scheme on IEEE 33-bus network showed it can improve the losses of the lines and voltage of the buses. Besides, the protection coordination between the protective devices lost due to the presence of the RESs was restored by optimizing the settings of the digital DOCRs and DS-DOCRs. Finally, the protection coordination of the digital DOCRs and DS-DOCRs exhibited a faster operating time relative to the OCRs and DOCRs due to the flexibility in the settings of different parameters. In the present paper, in lines where fault current is one-sided, the digital DOCRs were used, while in lines where fault current is two-sided, the digital DS-DOCRs were employed in order to reduce the installation costs of the CT, PT, DS-DOCRs and DOCRs. Based on the presented results, this issue showed the capability of GA algorithm in achieving loss reduction, voltage profile improvement and total operating time reduction of digital DOCR relays and digital DS-DOCR relays compared to PSO algorithm. According to the optimization results provided by GA and PSO, the following numerical results were obtained for each stage of the proposed design using GA:

- The optimization results showed the location and size of RESs in PV and WT at buses 30 and 17 were “469 kW of active power and 315 kVAR of reactive power” and “671 kW of active power and 340 kVAR of reactive power”, respectively.
- The optimization results indicated the location and size of SFCLs in PV, WT, line 8 and line 19 were 51.51 Ω , 29.46 Ω , 14.5 Ω and 8.6 Ω , respectively.
- The optimization results revealed the total operation time of relays was 36.321 sec.

REFERENCES

- [1] M. Alilou, D. Nazarpour, H. Shayeghi, “Multi-Objective Optimization of Demand Side Management and Multi DG

- in the Distribution System with Demand Response” *J. Oper. Autom. Power Eng.*, Volume 6, Issue 2, Pages 230-242, 2018.
- [2] S. Ghobadpour, M. Gandomkar and J. Nikoukar, “Multi-Objective Function Optimization for Locating and Sizing of Distributed Generation Sources in Radial Distribution Networks with Fuse and Recloser Protection,” *J. Oper. Autom. Power Eng.*, vol. 9, no. 3, pp. 266-273. 2021.
- [3] G. Derakhshan, H. Shahsavari and A. Safari, “Co-Evolutionary Multi-Swarm PSO Based Optimal Placement of Miscellaneous DGs in a Real Electricity Grids Regarding Uncertainties,” *J. Oper. Autom. Power Eng.*, vol. 10, no. 1, pp. 71-79. 2022.
- [4] S. Ghaemi and K. Zare, “A new method of distribution marginal price calculation in distribution networks by considering the effect of distributed generations location on network loss,” *J. Oper. Autom. Power Eng.*, vol. 5, pp. 171-180, 2017.
- [5] M. Kazeminejad et al, “The effect of high penetration level of distributed generation sources on voltage stability analysis in unbalanced distribution systems considering load mode,” *J. Oper. Autom. Power Eng.*, vol. 7, pp. 196-205, 2019.
- [6] S. Chatterjee and S. Chatterjee, “Review on the techno-commercial aspects of wind energy conversion system,” in *IET Renewable Power Gener.*, vol. 12, no. 14, pp. 1581-1608, 29 10 2018.
- [7] M. Usama, M. Moghavvemi, H. Mokhlis, N. N. Mansor, H. Farooq and A. Pourdaryaei, “Optimal Protection Coordination Scheme for Radial Distribution Network Considering ON/OFF-Grid,” in *IEEE Access*, vol. 9, pp. 34921-34937, 2021.
- [8] E. Purwar, D.N. Vishwakarma, S.P. Singh, “A novel constraints reduction-based optimal relay coordination method considering variable operational status of distribution system with DGs,” *IEEE Trans. Smart Grid*, vol. 10, no. 1, pp. 12-22, 2019.
- [9] P. Omidi, S. Abazari and S. M. Madani, “Optimal coordination of directional overcurrent relays for microgrids using hybrid interval linear programming - differential evolution”, *J. Oper. Autom. Power Eng.*, vol. 10, No. 2, pp. 122-133. 2022.
- [10] Asefi, S. Shayeghi, H. Shahryari, E. dadkhah, rashid, “Optimal management of renewable energy sources considering split-diesel and dump energy,” *Int. J. Techn. Phys. Prob. Eng. (IJTPE)*. 10. 34-40. (2018).
- [11] A. Q. Huang, “Power Semiconductor Devices for Smart Grid and Renewable Energy Systems,” in *Proce. IEEE*, vol. 105, no. 11, pp. 2019-2047, Nov. 2017.
- [12] Saman Ghobadpour, Majid Gandomkar, Javad Nikoukar, Determining Optimal Size of Superconducting Fault Current Limiters to Achieve Protection Coordination of Fuse-Recloser in Radial Distribution Networks with Synchronous DGs, *Electric Power Systems Research*, vol. 185, 106357, 2020.
- [13] J. Feng, B. Zeng, D. Zhao, G. Wu, Z. Liu and J. Zhang, “Evaluating Demand Response Impacts on Capacity Credit of Renewable Distributed Generation in Smart Distribution Systems,” *IEEE Access*, vol. 6, pp. 14307-14317, 2018.
- [14] M. Faghihi Rezaei, M. Gandomkar, and J. Nikoukar, “Optimal Protection Coordination of Dual-Setting Digital Directional Over-Current Relays with Renewable Resources and Energy Storage System”, *J. Novel Researches Elec. Power*, vol. 10, no. 3, pp.43-52, 2021.
- [15] M. Dashtdar, M. Najafi and M. Esmaeilbeig, “Reducing LMP and resolving the congestion of the lines based on placement and optimal size of DG in the power network using the GA-GSF algorithm,” *Electri. Eng.*, 2021.
- [16] H. Shad, M. Gandomkar, and J. Nikoukar. “An Improved Optimal Protection Coordination for Directional Overcurrent Relays in Meshed Distribution Networks with DG Using a Novel Truth Table,” *J. Oper. Autom. Power Eng.*, 2022.
- [17] H. Eid, H. M. Sharaf and M. Elshahed, “Optimal Coordination of Directional Overcurrent Relays in Interconnected Networks

- utilizing User- Defined Characteristics and Fault Current Limiter," *IEEE PES/IAS PowerAfrica*, pp. 1-5, 2021.
- [18] W. K. A. Najy, H. H. Zeineldin and W. L. Woon, "Optimal Protection Coordination for Microgrids With Grid-Connected and Islanded Capability," *IEEE Trans. Indu. Electron.*, vol. 60, no. 4, pp. 1668-1677, April 2013.
- [19] S. Abrisham Foroushan Asl , M. Gandomkar , J. Nikoukar, "System Stability-Constrained Optimal Protection Coordination in the Microgrid Including Renewable Energy Sources and Energy Storage," *JEM* 2021; 11 (2) :16-31.
- [20] E. Naderi, A. Dejamkhooy, S.J. Seyedshenava and H. Shayeghi, "MILP based optimal design of hybrid microgrid by considering statistical wind estimation and demand response," *J. Oper. Autom. Power Eng.*, vol. 10, no. 1, pp. 54-65. 2022.
- [21] M. N. Alam, "Adaptive Protection Coordination Scheme Using Numerical Directional Overcurrent Relays," *IEEE Trans. Indus. Informatics*, vol. 15, no. 1, pp. 64-73, 2019.
- [22] C. W. So and K. K. Li, "Time coordination method for power system protection by evolutionary algorithm," *IEEE Trans. Indu. Appli.*, vol. 36, no. 5, pp. 1235-1240, Sept.-Oct. 2000.
- [23] K. Jia, Z. Yang, Y. Fang, T. Bi, M. Sumner, "Influence of Inverter-Interfaced Renewable Energy Generators on Directional Relay and an Improved Scheme," *IEEE Trans. Power Electron.*, vol. 34, no. 12, pp. 11843-11855, Dec. 2019.
- [24] A. Arafa, M. M. Aly and S. Kamel, "Impact of Distributed Generation on Recloser-Fuse Coordination of Radial Distribution Networks," *Int. Conf. Innova. Trends Computer Eng. (ITCE)*, Aswan, Egypt, pp. 505-509, 2019.
- [25] Azizian, D., Bigdeli, M., Faiz, J.: 'Design optimization of cast-resin transformer using nature inspired algorithms', *Arab. J. Sci. Eng.*, vol. 41, no. 9, pp. 3491–3500, 2016.
- [26] J. Aghaei, M. Barani, M. Shafie-khah, A.A.S.d.l. Nieta, and J.P.S. Catalão, "Risk-constrained offering strategy for aggregated hybrid power plant including wind power producer and demand response provider," *IEEE Trans. Sustain. Energy*, vol. 7, no. 2, pp. 513-525, 2016.
- [27] M.F. Rezaei, M. Gandomkar, & J. Nikoukar, "Multi-Objective Function Optimization for Locating and Sizing of Renewable Energy Sources and Energy Storages in Radial Distribution Networks with Digital Digital Directional Overcurrent Relays and Digital Dual-Setting Directional Overcurrent Relays," *J. Electr. Eng. Technol.*, 17, 2095-2105, 2022.